Fire Suppression Modeling with Computational Fluid Dynamics: State of the Art

Meredith K.V.

Research Division, FM Global, Norwood, Massachusetts, USA
karl.meredith@fmglobal.com

ABSTRACT

An overview of the development and application of state-of-the-art fire suppression modeling is described herein. This begins with the identification of the key physics in fire suppression. A brief description of the submodel development and small-scale validation is included. These submodels, when merged together warrant large-scale validation. Finally, the combined model is used to simulate several practical, industrial-scale scenarios, examples of which are given.

KEYWORDS: CFD, fire modeling, fire suppression.

INTRODUCTION

Fire modeling is a tool that has been used effectively for several decades [1], providing great value to the fire protection engineering community. Early models relied on many simplifications, correlations, and empiricism, such as found in two-zone models, e.g. [2]. The rise in high performance computing (HPC) has led to a shift in the current state-of-the-art fire modeling approach towards physics-based computational fluid dynamics (CFD). CFD-based fire models excel at capturing flow dynamics in complicated geometries. As such, these models have found the most success in simulating the fire plume and the resultant transport of smoke, e.g. [3].

Continued progress in CFD modeling has resulted in the ability to simulate ever more complex scenarios. Most modern, general purpose CFD codes (e.g., ANSYS Fluent and Star-CCM+) can be useful in modeling basic fire related phenomena (gas-phase combustion [4], plume and ceiling jet dynamics [5, 6], etc.). Specialized fire-modeling codes (e.g. FDS [7]) have incorporated many fire-specific submodels, such as design-fire specification, solid-fuel pyrolysis, and sprinkler spray, etc. Unfortunately, both general purpose and specialized CFD codes have been of limited use with regards to water-based fire suppression modeling. This is because the key physics related to role of water in the suppression processes are missing.

Recently, FireFOAM [8, 9] has been developed with the goal of simulating fire suppression from first principles. FireFOAM includes key physics related to fire dynamics [9], heat transfer [10, 11], and soot/radiation [12]. FireFOAM also includes models for solid-phase pyrolysis [13]. These physical models have been used to simulate the intermediate-scale fire growth between parallel panels [14], and the large-scale rack-storage [15] and roll-paper [16] fire growth. This initial framework laid the foundation for introducing the effects of water and, thereby, simulating fire suppression.

Proceedings of the Ninth International Seminar on Fire and Explosion Hazards (ISFEH9), pp. 65-75
Edited by Snegirev A., Liu N.A., Tamanini F., Bradley D., Molkov V., and Chaumeix N.
Published by St. Petersburg Polytechnic University Press
ISBN: 978-5-7422-6496-5 DOI: 10.18720/spbpu/2/k19-137

DEVELOPMENT OF FIRE SUPPRESSION MODELING

In the simulation of water-based fire suppression, additional processes are relevant and robust submodels to treat these processes are needed. Specifically, the following physics need to be accurately modeled: sprinkler activation, sprinkler atomization, spray transport, spray impingement, thin-film transport, interfacial heat and mass transfer, gas-phase suppression due to evaporation and cooling from water spray, and radiation attenuation by sprays, etc. Many of these processes are depicted in Fig. 1a. Each of these submodels will be addressed in turn, along with available separate effect validation. Coupling these submodels together yields a robust platform fire suppression modeling.

Suppression submodels

The sprinkler activation model was implemented following the work of Heskestad and Bill [17], and is a function of the local gas-phase temperature and velocity, as shown in Eq. (1):

$$\frac{d(\Delta T_e)}{dt} = \frac{u^{1/2}}{\mathrm{RTI}}\left[\Delta T_g - \left(1 + \frac{C}{u^{1/2}}\right)\Delta T_e\right] \quad (1)$$

where ΔT_e is the temperature rise of the sprinkler thermal element, t is time, u is the gas-phase velocity magnitude, C is the conduction loss parameter, ΔT_g is the gas temperature relative to ambient temperature, and RTI is the response time index of the sprinkler. Once the sprinkler thermal element rises to a value above the activation temperature, the sprinkler will operate.

The sprinkler spray atomization model was implemented using a hemispherical injection model based on near-field experimental measurements [18]. The injection model utilizes measurements of liquid volume flux (an example of which is shown in Fig. 1b), droplet diameter, and droplet velocity as a function of azimuthal and elevation angles [19].

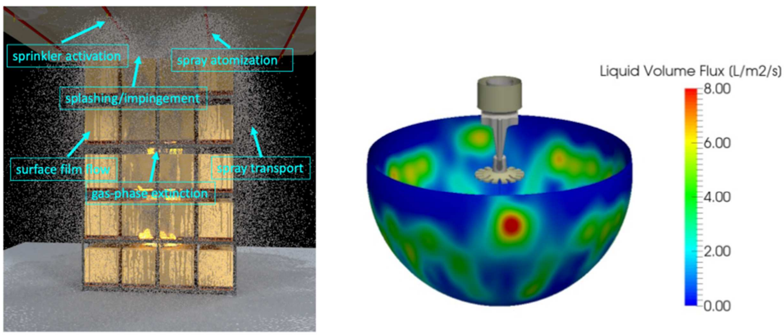

(a) (b)

Fig. 1. (a) Key phenomena related to fire growth and suppression. (b) Liquid volume flux measured at a radial distance of 12 cm (i.e., near-field) of a sprinkler [19].

The injection model introduces Lagrangian particles on this hemispherical surface in a fashion so as to ensure the liquid volume flux measurements are reproduced, initializes the particle velocity to the measured value, and randomly samples for particle diameter from a Rosin-Rammler distribution so as to match the measured mean volume diameter of the spray.

The spray transport model utilizes the existing Lagrangian-particle transport model within OpenFOAM [20]. Heat transfer, mass transfer, and momentum transfer models have been validated [21] against detailed spray-plume interaction measurements [22]. An example of the comparison between the measured velocity field for a spray-plume interaction is shown in Fig. 2 for increasing plume strengths for a fixed spray condition. As the plume strength increases, the stagnation region between the spray and the plume is pushed further downstream.

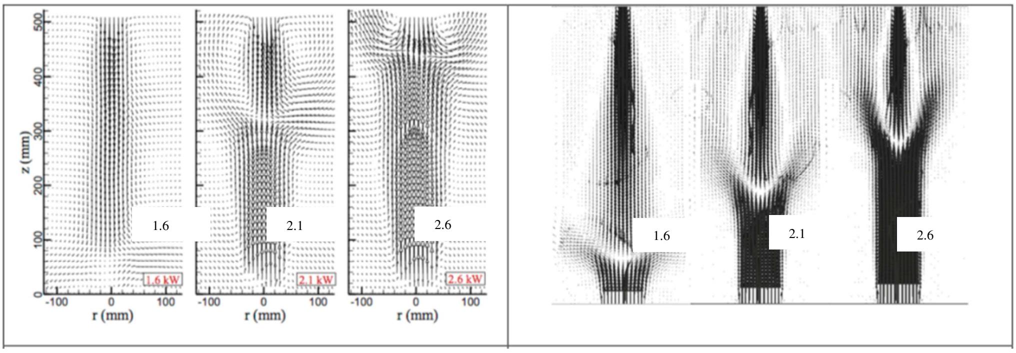

(a) experimental measurements (b) simulations

Fig. 2. Velocity comparisons for thermal plumes of 1.6, 2.1, and 2.6 kW convective strength [21].

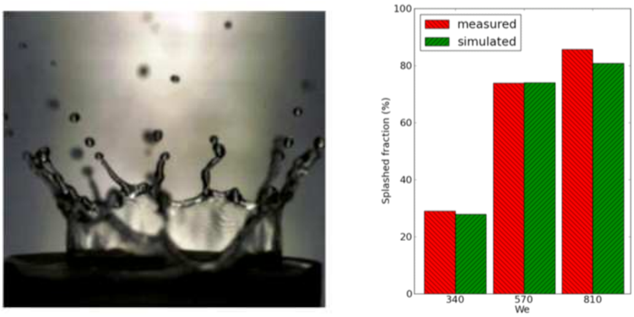

(a) (b)

Fig. 3. (a) A splashing event captured 15 ms after impact for We = 810; (b) splash mass fraction comparisons for three Weber numbers [23].

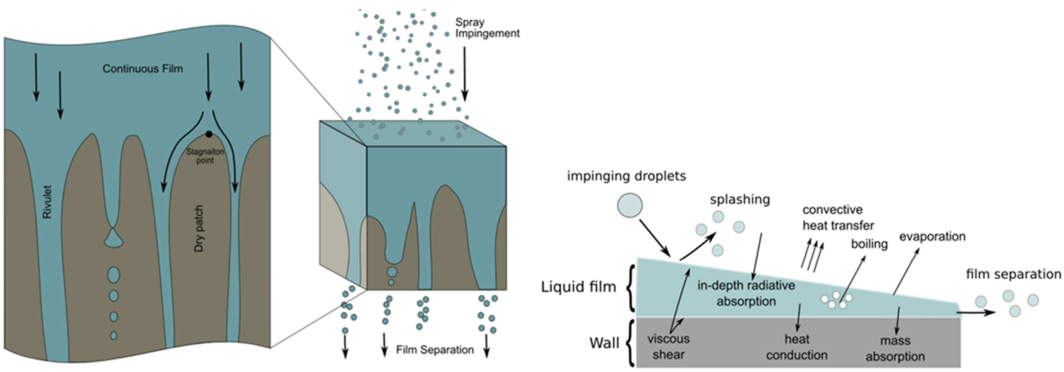

Fig. 4. Thin-film water transport model, encapsulating partial wetting (e.g., rivulet flow) and interfacial transport phenomena.

A model is needed to treat the interaction of the spray with solid surfaces. The spray can either absorb onto the surface (creating a thin liquid film) or can splash (resulting in the ejection of many small, high-speed droplets). A model to treat spray impingement has been implemented [23] that, as a function of Weber number, determines the type of interaction at the surface. Based on this model, the impinging droplet can adhere, bounce or splash. The model has been compared to experimental measurements for splashing behavior. An example of such is shown in Fig. 3.

Once the spray has impinged and adhered to the surface, a thin film will be formed. This thin film can transport over the surface. To capture the physics of thin film flow (as depicted in Fig. 4), a model has been developed and implemented [24]. This model considers partially-wetted flow, namely the formation of dry patches and rivulets due to contact angle forces. Simplifications were made based on the thin-film assumption [25] that allowed for a two-dimensional representation, thereby greatly reducing the computational cost while still adequately capturing the main physics. The model also considers interfacial mass, momentum, and heat transfer such as evaporation/boiling, viscous shear stresses, and convective/radiative heat transfer, the physics of which are represented schematically.

The thin-film model has been verified and validated against the Nusselt solution [25] for thin film flows and also against experimental measurements [26], as is shown in Fig. 5 for various surface inclination angles.

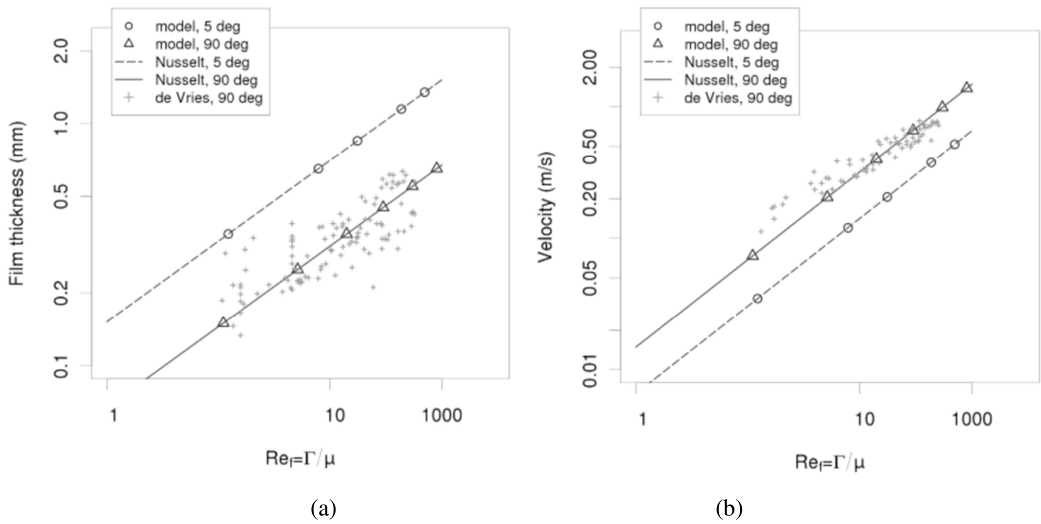

Fig. 5. Comparisons of film model with Nusselt solution and experimental data: (a) film thickness; (b) velocity.

A model for partially-wetted flow was added to the film model to simulate rivulet formation and continuous-film flow [26]. Partially wetted flow behavior entails flow delineated by a contact line separating the dry and wet surfaces, which takes the form of rivulets, dry patches, and isolated wet spots. These effects were introduced in the model as a contact-angle force term that acts along the contact line delineating the separation of wet and dry regions of the flow. This surface-tangential force limits the film from spreading, and reproduces the partially wetted flow behavior. For a given contact angle a film will exhibit a minimum or critical film thickness. Below this thickness, the film will not be able to flood the surface but will be balanced by the contact angle force. Validation of the partially-wetted flow model was performed by comparing with experimental measurements of film flow on an incline surface, as shown in Fig. 6. At high flow rates, the film spreads out and tends to flood the surface. As flow rate decreases (from right to left), the film undergoes a transition to rivulet flow. The model reproduces this behavior.

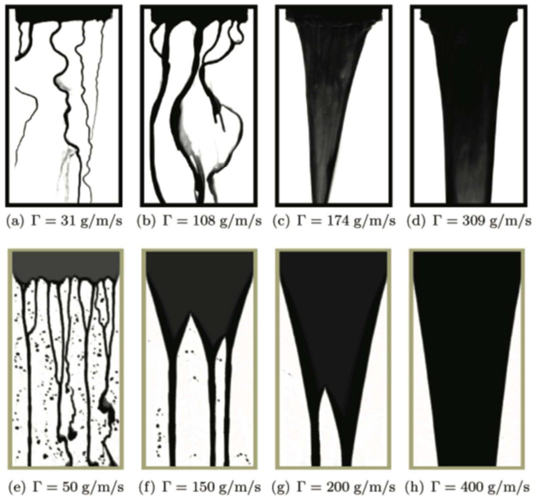

Fig. 6. Experimental film flow (a–d) compared with simulated film flow (e–h) (5° incline) [26].

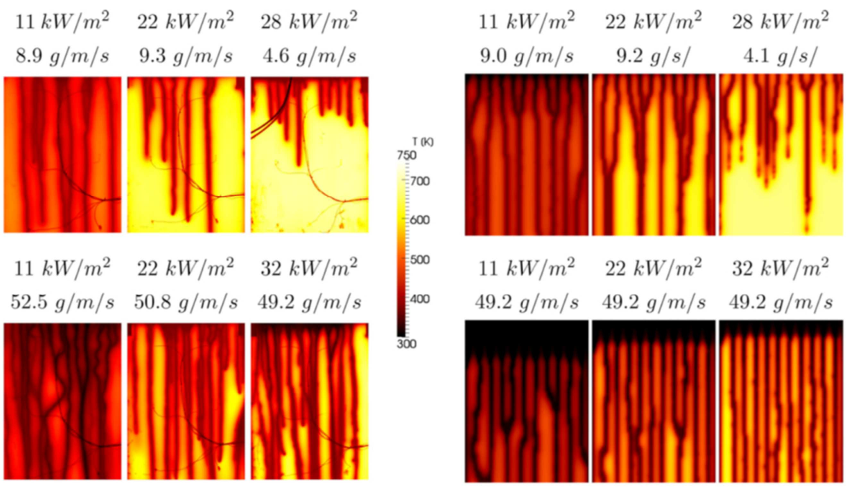

a) experimental measurements b) model predictions

Fig. 7. Comparisons of the thin-film model results with experimental measurements for surface temperature on a thin, steel plate. The film is shown by the low temperature regions [28].

A phenomenon that has been shown to be important in fire suppression scenarios is the thermocapillary (or Marangoni) stress on the liquid film caused by spatially varying heating rates and film thicknesses [27]. Dry regions are formed on the surface as the film pulls together as rivulets. the high surface tension near the center of the rivulet (at a lower temperature) pulls the lower surface tension fluid near the rivulet edge (at a higher temperature) towards the center. A model for the effect of thermocapillary stress was implemented [27]. This model, along with a model for the conjugate heat transfer between the gas-, liquid-, and solid-phases was compared with experimental data [28]. The results show validation for the heat transfer, vaporization, and partially-wetted flow behavior of the thin film model, as shown in Fig. 7. These experiments and simulations imposed a given radiant heat flux on the surface of a vertical panel. The flow of a thin liquid film down the surface was validated by comparing temperature measurements, evaporation rates, and wetted area fractions.

The film model was applied to simulate the flow over rack-storage commodities [24], as shown in Fig. 8. As in the vertical panel simulations, when the flow rate is low rivulets are formed. During fire suppression, these dry patches have the potential to allow for easier fire spread within the rack storage array.

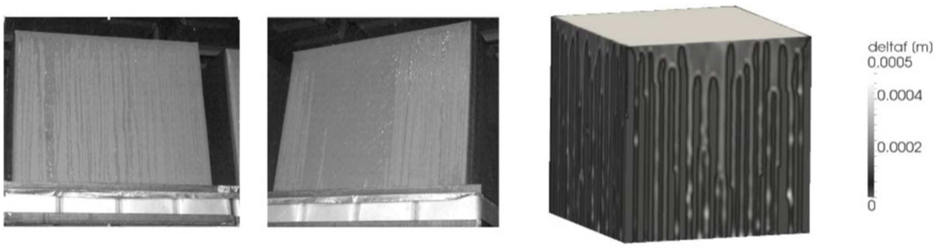

Fig. 8. Qualitative comparisons of experiment and model predictions for film thickness on a cardboard box with an applied water flux to the top surface of 4 L/(min·m^2) [24].

Additionally, the film model was validated for the flow of water over a more complex-shaped commodity for scenarios where the sprinkler is placed directly within the storage array (i.e., an in-rack sprinkler configuration) [29]. An example of the resulting predictions for film thickness are shown in Fig. 9a for an uncartoned, expanded plastic commodity (UEP), whereas comparisons with experimental measurements of collected water at the base of the array are shown in Fig. 9b. The predictions for the spatial distribution of the flow at the base of the array matched well with the experimentally measured values.

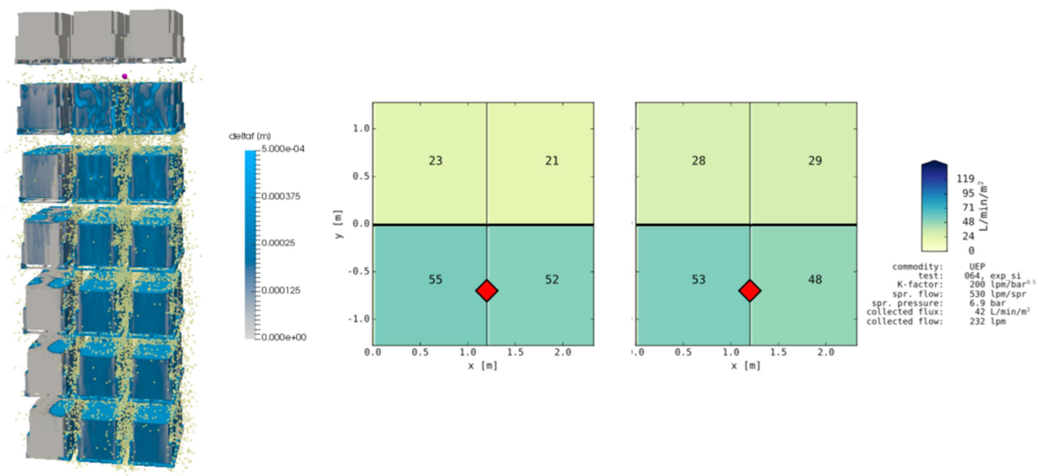

(a) (b)

Fig. 9. a) Contours of film thickness (blue) on a complex commodity (UEP) surface (grey) at 100 s after sprinkler (purple dot) operation. b) Comparison collected water flux at the base of the array; the red diamond represents the sprinkler location.

Two other separate-effect physics have been included in FireFOAM to enable accurate simulation of fire suppression. First, an additional submodel was needed to treat gas-phase extinction in oxygen-reduced environments [30]. This model treats the interactions of the non-premixed flame with flow turbulence. Turbulence can disturb the flame surface and initiate mixing between fuel, air, and combustion products. Near extinction, pockets of pre-mixture in the form of mixed eddies can be formed. The evolution of such a mixed eddy is determined by the competition of the heat release and heat loss rates, which are linked to the eddy size, the local flame thickness, and the turbulent Karlovitz number. Radiation from the reacting flame sheet is modeled considering the gaseous combustion products and soot. The model was evaluated using gaseous-pool fires in an enclosure with CH_4, C_3H_8 and C_2H_4 diluted with nitrogen in air flow. The model predictions compared favorably with test data for combustion efficiency, flame height and global radiant fraction.

Secondly, a radiation attenuation due to interaction with sprays has also been included [31]. Accurate numerical models were needed to better understand radiative heat transfer process in water-based suppression scenarios. To that end, a Mie-theory based model for radiation attenuation by water droplets has been developed and implemented in FireFOAM. This wide-band model has been formulated for absorption and scattering by water droplets. The absorption and scattering efficiencies (calculated from Mie theory), and the phase function, are pre-tabulated to make the CFD calculations more efficient. The model employs an enhanced formulation for scattering with discrete solid angles to ensure energy conservation. The model results have been compared with theoretical data for a canonical configuration and with detailed Monte Carlo Ray Tracing (MCRT) calculations, and good agreement has been obtained.

Combined validation

A similar approach (i.e., development, verification, validation) was also taken for the fire-dynamics-related submodels and physics, such as reacting buoyant plumes [9], thermal radiation heat transfer from soot emission [12], and solid-phase pyrolysis [13]. The combined-effects, fire-dynamics submodels were validated for a rack-storage fire, where all above-mentioned submodels are combined to produce results that need to match quantities such as global heat release rate, flame spread pattern, local heat flux and temperature, etc. Fig. 10 shows the simulation results for rack storage of Class 2 commodity [32] (corrugated cardboard boxes on a hardwood pallet with a metal liner inside). The simulations demonstrated the ability of the fire growth model to reproduce the vertical and lateral flame spreads for different storage heights and footprint sizes.

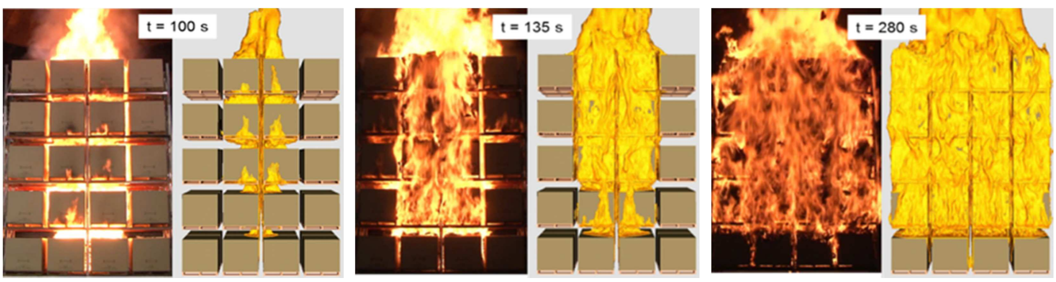

Fig. 10. Experimental and simulated rack-storage fire growth for 5-tier high, Class 2 commodity [32].

These models, combined with the suppression-related submodels, were validated by comparing to a series of rack-storage suppression cases [15, 32]. An example of this validation is shown in Fig. 11. Test snapshots are also shown alongside the simulated suppression cases. Shown in Fig. 12, the simulation can predict the heat release rate of the free-burn case, and the fire suppression response when water is applied for a 3-tier high storage scenario and a 5-tier high storage scenario. The comparisons for model prediction with free-burn and suppression experiments demonstrates that the current CFD model captures major physics important for Class 2 commodity fires.

Still, there are many outstanding challenges in simulating practical, industrial-scale fire suppression. One challenge relates to improving the existing suppression submodels to account for more real-world effects such as sprinkler skipping. Another challenge is treating complex fuels (i.e., solid fuels made up of more than one material). For example, simulating a commodity such as cartoned, unexpanded plastic (CUP) is more challenging because the interior of the commodity also contains combustible material. While the existing fire modeling framework has been extended to cover a commodity such as CUP [33], further work related to coupling the suppression models with the interior contents of the commodity is needed. In general, dealing with changing geometries (e.g., due to burnout, deformation, delamination, melting, etc.) is still illusive for CFD modeling in general. More effort is needed on this front. Finally, improving the model fidelity while at the same time maintaining a tractable solution time can be difficult. Efforts on this front related to adaptive mesh refinement, improved parallel efficiency, and dynamic load balancing are needed.

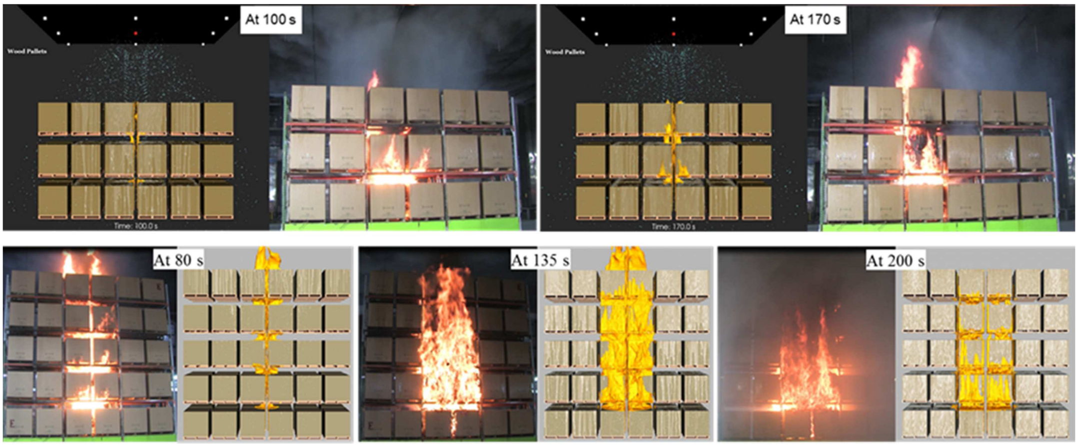

Fig. 11. Snapshots showing comparison between test and simulation of 3-tier (top) and 5-tier (bottom) high rack-storage array; white color on the boxes shows the water film flow cases [15, 32].

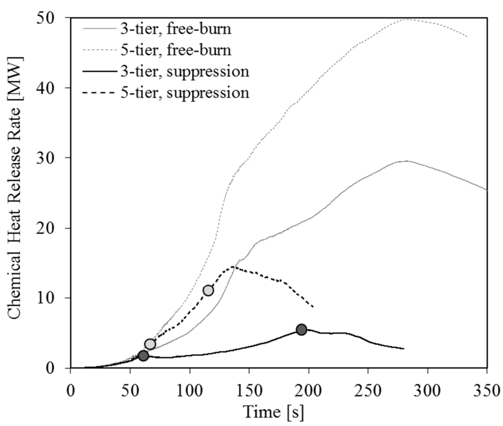

Fig. 12. Simulated heat release rates for both free-burn and suppression cases; symbols indicate the first two sprinkler activation times [15].

Applied suppression modeling

The combined suppression model has been applied to simulate other realistic scenarios, allowing simulations, coupled with testing, to provide guidance on protection solutions. Recently, the suppression model was extended to simulate roll-paper fire protection [16]. This application required the development of a specialized pyrolysis model to handle roll-paper specific phenomena, such as delamination, peeling, and the corresponding heat transfer mechanism. Detailed injection models for large K-factor sprinklers were used to simulate the injection of the sprinkler spray. The thin-film model was coupled with the pyrolysis model to simulate the cooling of the pyrolyzing surfaces, thus determining the suppression response. The model validation was performed by comparing with a series of roll-paper fire tests with ceiling at 18.3-m high and different storage heights. The validated model was then used to evaluate the design options for even higher roll paper storages, scenarios that are difficult to testing directly. Figure 13 demonstrates the full modeling capability for this configuration, ranging from immediately following sprinkler activation to the suppression state.

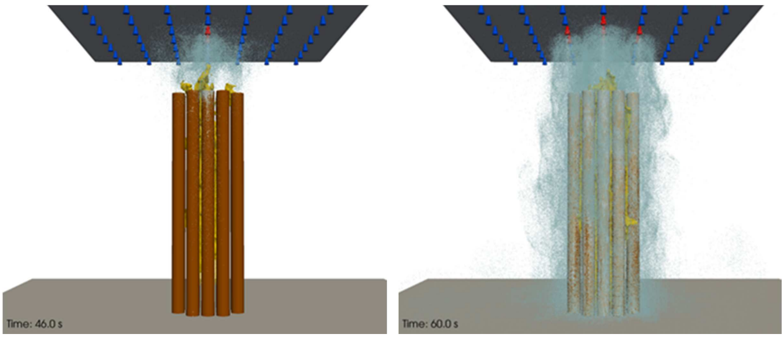

(a) (b)

Fig. 13. Simulated fire suppression of roll-paper storage at a) just after sprinkler activation, and b) after sufficient time for suppression to begin to take effect.

Other applications of this suppression model for practical scenarios have been in the areas of complex fuels (e.g., cartoned unexpanded plastics) [33], sloped ceilings [34], and in-rack sprinklers [29].

CONCLUSIONS

A state-of-the-art model for simulating fire-suppression has been developed and coupled with well validated fire dynamics models. The suppression models include sprinkler activation, spray transport, thin-film flow, gas-phase extinction, and radiation attenuation due to sprays. These models have been separately validated. The combined model has been used to simulate rack-storage suppression and validated against full-scale test results. The model has been extended and applied to simulate practical industrial fire protection scenarios such as roll-paper storage.

Although fire-suppression modeling has progressed to a certain level of maturity, the fidelity of the modeling will continue to be enhanced and extended to additional scenarios. With the new capabilities, fire-suppression modeling will evolve to be a powerful tool for industrial fire protection to complement fire testing and lead to improved protection solutions in a more expedited and cost-effective manner.

ACKNOWLEDGEMENTS

The work discussed herein was funded by FM Global and performed within the framework of the FM Global Strategic Research Program on Fire Modeling. The author would like to thank the many collaborators within FM Global, namely Drs. Ning Ren, Prateep Chatterjee, Jaap de Vries, Xiangyang Zhou, Ankur Gupta, Alex Krisman, Luwi Oluwole, Yi Wang, and Sergey Dorofeev for their contributions to this work. Also, collaborators in the OpenFOAM community, namely Andy Heather, are acknowledged for their developments on the underlying framework for the thin-film model.

REFERENCES

[1] S.M. Olenick, D.J. Carpenter, An Updated International Survey of Computer Models for Fire and Smoke, J. Fire Protect. Eng. 13 (2003) 87-110.

[2] D.M. Brani, W.Z. Black, Two-zone model for a single-room fire, Fire Saf. J. 19 (1992) 189-216.

[3] S. Simcox, N.S. Wilkes, I.P. Jones, Computer simulation of the flows of hot gases from the fire at King's Cross Underground station, Fire Saf. J. 18 (1992) 49-73.

[4] H. Xue, J.C. Ho, Y.M. Cheng, Comparison of different combustion models in enclosure fire simulation, Fire Saf. J. 36 (2001) 37-54.

[5] T.G. Ma, J.G. Quintiere, Numerical simulation of axi-symmetric fire plumes: accuracy and limitations, Fire Saf. J. 38 (2003) 467-492.

[6] K. Van Maele, B. Merci, Application of two buoyancy-modified k–ε turbulence models to different types of buoyant plumes, Fire Saf. J. 41 (2006) 122-138.

[7] Fire Dynamics Simulator. [cited 2017 March 3]; Available from: www.fire.nist.gov.

[8] FireFOAM. 2017; Available from: http://www.fmglobal.com/research-and-resources/research-and-testing/theoretical-computational-and-experimental-research/open-source-fire-modeling.

[9] Y. Wang, P. Chatterjee, J.L. de Ris, Large eddy simulation of fire plumes, Proc. Combust. Inst. 33 (2011) 2473-2480.

[10] N. Ren, Y. Wang, S. Vilfayeau, A. Trouvé, Large eddy simulation of turbulent vertical wall fires supplied with gaseous fuel through porous burners, Combust. Flame 169 (2016) 194-208.

[11] Y. Wang, K. Meredith, X. Zhou, P. Chatterjee, Y. Xin, M. Chaos, N. Ren, S. Dorofeev, Numerical Simulation of Sprinkler Suppression of Rack Storage Fires, In: Fire Safety Science – Proceedings of the Eleventh International Symposium, pp. 1170-1183, 2014.

[12] P. Chatterjee, J.L. de Ris, Y. Wang, S.B. Dorofeev, A Model for Soot Radiation in Buoyant Diffusion Flames, Proc. Combust. Inst. 33 (2011) 2665-2671.

[13] M. Chaos, M.M. Khan, S.B. Dorofeev, Pyrolysis of corrugated cardboard in inert and oxidative environments, Proc. Combust. Inst. 34 (2012) 2583-2590.

[14] N. Krishnamoorthy et al., Application of Bench-Scale Material Flammability Data to Model Flame Spread in Medium- Scale Parallel Panel Test, In: Proceedings of the 12th Fire Science and Engineering Conference, INTERFLAM, Nottingham, UK, pp. 709-720, 2010.

[15] N. Ren, J. de Vries, X. Zhou, M. Chaos, K.V. Meredith, Y. Wang, Large-scale fire suppression modeling of corrugated cardboard boxes on wood pallets in rack-storage configurations, Fire Saf. J. 91 (2017) 695-704.

[16] N. Ren, D. Zeng, K.V. Meredith, M. Chaos, Y. Wang, S.B. Dorofeev, CFD Modeling of Industrial-Scale Roll-Paper Fires, In: 8th International Seminar on Fire and Explosion Hazards, Hefei, China, 2016.

[17] G. Heskestad, J.R.G. Bill, Quantification of Thermal Responsiveness of Automatic Sprinklers Including Conduction Effects, Fire Saf. J. 14 (1988) 113-125.

[18] X. Zhou, S.P. D'Aniello, H.Z. Yu, Spray characterization measurements of a pendent fire sprinkler, Fire Saf. J. 54 (2012) 36-48.

[19] K.V. Meredith et al., VOF Modeling of Fire Sprinkler Spray Patternation, In: 13th International Conference on Liquid Atomization and Spray Systems, Tainan, Taiwan, 2015.

[20] G.B. Macpherson, N. Nordin, H.G. Weller, Particle tracking in unstructured, arbitrary polyhedral meshes for CFD and molecular dynamics, In: Communications in Numerical Methods in Engineering, 2008.

[21] K.V. Meredith et al., Numerical Simulation of Spray-Plume Interactions, In: 9th U.S. National Combustion Meeting, Cincinnati, OH, 2015.

[22] X. Zhou, Characterization of interactions between hot air plumes and water sprays for sprinkler protection, Proc. Combust. Inst. 35 (2015) 2723-2729.

[23] K.V. Meredith, X. Zhou, A. Heather, A Spray Interaction Model with Application to Surface Film Wetting, In: 12th International Conference on Liquid Atomization and Spray Systems, 2012.

[24] K.V. Meredith, Y. Xin, J. de Vries, A Numerical Model for Simulation of Thin-Film Water Transport over Solid Fuel Surfaces, In: Fire Safety Science – Proceedings of the Tenth International Symposium, pp. 415-428, 2011.

[25] W. Nusselt, Die Oberflachenkondensation des Wasserdampfes, Zeitschrift des Vereines Deutscher Ingenieure, 60 (1916) 541-546 and 569-575-541.

[26] K.V. Meredith et al., A numerical model for partially-wetted flow of thin liquid films, In: Computational Methods in Multiphase Flow, Vol. VI, pp. 239-250, 2011.

[27] K.V. Meredith, J. de Vries, Rupture of Thin Liquid Films under the Influence of External Heat Flux, In: 7th International Conference on Computational and Experimental Methods in Multiphase and Complex Flow, La Coruna, Spain July 3-5, 2013.

[28] K.V. Meredith et al., A comprehensive model for simulating the interaction of water with solid surfaces in fire suppression environments, Proc. Combust. Inst. 34 (2013) 2719-2726.

[29] K.V. Meredith, J. De Vries, X. Zhou, Y. Wang, Simulating the interaction of spray and surface film flow with complex geometries in fire suppression applications, In: International conference on multiphase flow, 2016.

[30] N. Ren, D. Zeng, K.V. Meredith, Y. Wang, S.B. Dorofeev, Modeling of flame extinction/re-ignition in oxygen-reduced environments, Proc. Combust. Inst. 37 (2019) 3951-3958.

[31] A. Gupta, K.V. Meredith, Y. Wang, Models for Absorption and Scattering of Radiation by Water Droplets in Fire Suppression Environments, In: 10th U.S. National Combustion Meeting, College Park, Maryland, Eastern States Section, Combustion Institute, 2017.

[32] N. Ren, J. de Vries, K.V. Meredith, M. Chaos, Y. Wang, FireFOAM Modeling of Standard Class 2 Commodity Rack Storage Fires, In: Proceedings of Fire and Materials Conference, San Francisco CA, 2015.

[33] A. Gupta et al., Modeling of Large-Scale Fires in Cartoned Plastic Commodity Rack-Storage in INTERFLAM, Royal Holloway College, Nr Windsor, UK, 2016.

[34] P. Chatterjee, Sprinkler Performance under Non-Sloped Obstructed Ceiling Construction, FM Global, 2018 (published online).